LJMU Research Online

Salaris, M and Bedin, LR

 Praesepe white dwarfs in Gaia DR2

http://researchonline.ljmu.ac.uk/id/eprint/10973/

Article

For more information please contact researchonline@ljmu.ac.uk

Praesepe white dwarfs in *Gaia* DR2

M. Salaris[1]★ and L. R. Bedin [2]★

[1]*Astrophysics Research Institute, Liverpool John Moores University,146 Brownlow Hill, Liverpool L3 5RF, UK*
[2]*Istituto Nazionale di Astrofisica – Osservatorio Astronomico di Padova, Vicolo dell'Osservatorio 5, I-35122 Padova, Italy*

ABSTRACT

We have exploited *Gaia* Data Release 2 to study white dwarf members of the Praesepe star cluster. We recovered 11 known white dwarf members (all DA spectral type) plus a new cluster WD never identified before. 2 of the 11 known DA objects did not satisfy all quality indicators available in the data release. The remaining nine objects of known spectral type have then been employed to determine their masses (average error of 3–5 per cent) and cooling times (average uncertainty of 5–7 per cent), by fitting cooling tracks to their colour–magnitude diagram. Assuming the recent *Gaia* Data Release 2 reddening and main-sequence turn-off age estimates derived from isochrone fitting, we have derived progenitor masses and established the cluster initial–final mass relation. We found consistency with the initial–final mass relation we established for eight Hyades white dwarfs, also employing *Gaia* data. We have investigated also the effect on the derived initial masses of using self-consistently different sets of stellar models and isochrones for determining cluster age and white dwarf progenitor lifetimes. According to our established Hyades + Praesepe initial–final mass relation, recent sets of stellar evolution calculation that model the full asymptotic giant branch phase do on average underpredict the final white dwarf masses, in the initial mass range covered by the Praesepe and Hyades observed cooling sequence. These results depend crucially on the assumed reddening for the cluster. To this purpose, we have also discussed the case of considering the traditional zero reddening for Praesepe, instead of $E(B - V) = 0.027$ derived from isochrone fitting to the *Gaia* colour–magnitude diagram.

Key words: stars: evolution – stars: mass-loss – white dwarfs – open clusters and associations: individual: (Praesepe).

1 INTRODUCTION

Theoretical calculations of the relationship between the initial (main-sequence) mass and the final carbon–oxygen (CO) white dwarf (WD) mass for low- and intermediate-mass stars is still challenging. This stems from the poorly modelled efficiency of mass-loss in stellar model calculations, and uncertainties in the evolution of the mass size of CO cores during the asymptotic giant branch (AGB) phase (see e.g. Iben & Renzini 1983; Dominguez et al. 1996; Karakas & Lattanzio 2014).

This state of affairs is problematic, because the initial–final mass relation (IFMR) is an essential input for several astrophysical problems. Obviously, location and shape of cooling sequences in colour–magnitude diagrams (CMDs) and the associated WD luminosity functions – sometimes employed to age date stellar populations – are affected by the IFMR, but also chemical evolution histories of stellar populations, their mass-to-light ratios, modelling of stellar

feedback in galaxy formation simulations (e.g. Agertz & Kravtsov 2015), Type Ia supernova rate estimates (e.g. Greggio 2010) do depend on the choice of the IFMR.

To overcome these shortcomings of stellar evolution models, semi-empirical methods have been devised to establish the IFMR (see e.g. Weidemann 2000; Ferrario et al. 2005; Catalán et al. 2008; Kalirai et al. 2009; Salaris et al. 2009; Williams, Bolte & Koester 2009; Cummings et al. 2015, 2018, for recent examples).

Semi-empirical IFMR techniques are still largely based on WDs hosted by star clusters. Theoretical analyses of WD spectra provide surface gravity g and effective temperature T_{eff}, by simultaneous fitting of Balmer line profiles of DA WDs, employing high-resolution observed and synthetic spectra. For a given $g - T_{eff}$ pair, grids of theoretical WD models then provide the WD mass (M_f) and cooling age (t_{cool}).

At the same time, theoretical isochrone fits to the main-sequence (MS) turn-off luminosity of the cluster CMD give the cluster age (t_{cl}). The difference $t_{cl} - t_{cool}$ corresponds to the lifetime of the WD progenitor until the start of the WD cooling (t_{prog}). Finally, mass–lifetime relationships from theoretical stellar evolution tracks

provide an initial progenitor mass (M_i) from t_{prog} (the uncertain AGB and post-AGB lifetimes can be neglected, because their duration is negligible compared to the duration of the previous phases).

The high-precision astrometry and three-band photometry (G, G_{BP}, G_{RP}) of *Gaia* Data Release 2 (DR2) has enabled to build CMDs of the closest open clusters (Gaia Collaboration 2018) that display exquisitely defined sequences. The distance modulus corrected CMD of the Hyades cluster, for example, has typical errors (including the parallax error contribution) of a few mmag in all three filters, including the WD cooling sequence (see e.g. Salaris & Bedin 2018, hereafter Paper I).

Taking advantage of the DR2 parallaxes and photometry, in Paper I we have determined precise masses and cooling times (typically 1–3 per cent precision) of the eight confirmed DA WDs Hyades members, by fitting theoretical cooling tracks to the observed CMD. When absolute magnitudes and colours are accurately known, this technique works well, and is somewhat complementary to the spectroscopic one. In case of CMD fitting, theoretical WD cooling sequences are used in conjuction with – this time – low-resolution synthetic spectra, needed to calculate the appropriate bolometric corrections and colours.

The Hyades IFMR was then established from the knowledge of the cluster age determined from the MS turn-off by Gaia Collaboration (2018), employing the DR2 CMD. WDs in the Hyades cover a range of masses corresponding to M_i between ∼2.5 and ∼4.0 $M_\odot$, an *interesting* mass range from the point of view of stellar evolution. The lower limit corresponds approximately to stars just beyond the threshold for He-ignition in a non-degenerate core. This means that above ∼2.5 $M_\odot$ the He-core mass at the start of core He-burning starts to increase with increasing M_i (at lower masses the He-core mass at He-ignition is approximately constant with M_i because of the electron degeneracy). The upper limit of this mass range corresponds approximately to the onset of the second dredge-up during the early-AGB phase. The second dredge-up moderates the increase of M_f with increasing M_i. As a result, theoretical IFMRs predict for this initial mass range a steeper slope in the $M_i - M_f$ diagram, compared to lower and higher mass ranges (see e.g. predictions from models by Choi et al. 2016; Marigo et al. 2017).

In this paper we consider *Gaia* DR2 data for the Praesepe cluster – roughly coeval and with the same metallicity of the Hyades – that include a well-defined WD sequence. We apply the same techniques employed in Paper I to determine the cluster IFMR. Putting together the Hyades and Praesepe IFMR derived from the DR2 data, allows us to test theoretical IFMRs in this important M_i range. In Paper I we assessed the – negligible – effect on the WD masses and cooling times (and the derived IFMR) of employing three independent sets of WD cooling models. Here we explore the effect of employing independent sets of stellar evolution models/isochrones to determine progenitor masses, and their impact on the IFMR.

The plan of the paper is as follows. Section 2 describes briefly the Praesepe WD sample, whilst section 3 describes our derivation of the WD masses, cooling times, and comparisons with previous independent determinations. Section 4 presents our derivation of the IFMR with associated errors employing the cluster age and reddening determined from isochrone fitting to the *Gaia* MS and turn-off CMD, the effect of using different sets of stellar models/isochrones to determine M_i, and comparisons with theoretical IFMR predictions. In addition, we also rederive the IFMR using this time the recent cluster age determined from Johnson photometry by Cummings et al. (2018), considering the traditional zero reddening for this cluster. A summary and discussion follow in Section 5.
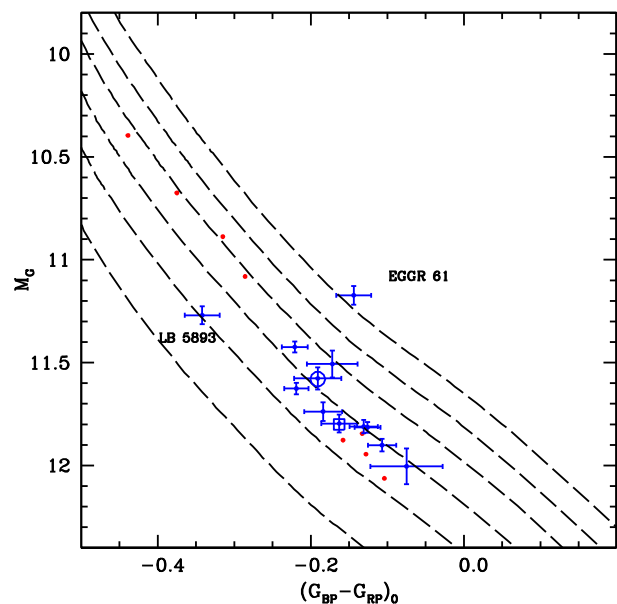

Figure 1. *Gaia* DR2 CMD – distance modulus and reddening corrected – of the sample of 12 Praesepe WD members (blue filled circles with error bars) together with the Salaris et al. (2010) H-atmosphere cooling tracks for masses equal to 0.54, 0.61, 0.68, 0.77, 0.87, and 1.00 $M_\odot$ (see text for details). Error bars include the DR2 quoted photometric errors and the contribution from the parallax error. The object enclosed within an open circle is a magnetic WD (see text). The object enclosed within an open square is a new member WD (see text for details). Filled red circles without error bars denote the Hyades WDs of Paper I. The two labelled Praesepe WDs are *peculiar* objects discussed in the text.

2 DATA

The 932 Praesepe members considered for this work are those defined and released by Gaia Collaboration (2018). We translated apparent G-band magnitudes and observed ($G_{BP} - G_{RP}$) colours to absolute magnitude and reddening-corrected colours employing the individual DR2 parallaxes, $E(B - V) = 0.027$ as derived (together with the age) from isochrone fitting by Gaia Collaboration (2018). We notice that this value agrees with the reddening determined by Taylor (2006); the associated formal error on Taylor (2006) determination is negligible, equal to 0.004 mag (see Section 4.1 for more on Praesepe reddening).

We have added to the published DR2 parallaxes a zero-point correction by 0.03 mas, following Lindegren et al. (2018). The effect of this correction on the absolute magnitudes is however almost negligible. Extinction coefficients for the three *Gaia* photometric filters have been derived as described in section 2.2 of Gaia Collaboration (2018) – see their equation (1).

The resulting cooling sequence in the *Gaia* CMD is displayed in Fig. 1. The 1σ error bars take into account both photometric and, for the absolute G-band magnitudes, parallax errors. Parallax fractional errors are typically around 4 per cent, while 1σ errors on M_G and colours are in the range 0.03–0.07 and 0.02–0.03 mag, respectively.

The sequence is populated by 12 WDs, 11 of which are already known cluster members (see Anthony-Twarog 1984; Claver et al. 2001; Dobbie et al. 2004, 2006; Casewell et al. 2009). These known members are all DA objects, and are all listed in the Montreal White Dwarf Data base (Dufour et al. 2017). Casewell et al. (2009) argued that one of these 11 objects (WD 0837+218) is possibly a non-member, but it is found to be a cluster member by Gaia

Collaboration (2018) in their analysis of star clusters in *Gaia* DR2. The new WD of unknown spectral type has the DR2 identifier #662998983199228032.

Fig. 1 shows also the Hyades cooling sequence of Paper I (red dots), as well as Salaris et al. (2010) theoretical DA WD cooling tracks, for masses M_{WD} between 0.54 and 1.0 M$_\odot$. The cooling tracks are calculated for CO cores (see Salaris et al. 2010, for details about the CO stratification) and thick H layers (mass thickness equal to $10^{-4}M_{WD}$, on top of a $10^{-2}M_{WD}$ He layer). The theoretical absolute magnitudes in the *Gaia* DR2 filter system were determined from the model bolometric luminosities by applying bolometric corrections kindly provided by P. Bergeron (private communication; see Holberg & Bergeron 2006; Tremblay, Bergeron & Gianninas 2011).

As expected, due to the cluster similar ages and metallicities (e.g. Gaia Collaboration 2018), Hyades and Praesepe WDs appear to follow a single cooling sequence, with the exception of the two labelled Praesepe objects. They are too blue (mass too high) and too red (mass too low) compared to the combined cooling sequence of the two clusters.

To investigate whether these peculiar colours are due to issues with DR2 data, we have checked the quality indicators available in *Gaia* DR2[1] for the whole sample of Praesepe WDs. As done in Paper I for the Hyades WDs, we have considered `visibility_periods_used`, `astrometric_matched_observations`, `astrometric_gof_al`, `astrometric_excess_noise`, `astrometric_n_good_obs_al`, `astrometric_n_bad_obs_al`, plus all the estimated errors on motions, positions, and magnitudes for all filters, and compared with their average values for magnitude intervals. Finally, we also inspected the tests for well measured objects defined in equations (C.1) and (C.2) of Lindegren et al. (2018).

All these indicators – for the whole WD sample – appear to be reasonably well measured, with the only exceptions of EGGR 60 (#661311267210542080) – the faintest object in Fig. 1 – and EGGR 61 (#661297901272035456). These objects did not pass the test defined by equation (C.2) of Lindegren et al. (2018) that flags problem with the G_{BP} and G_{RP} photometry. For this reason we would not consider these WDs in the analysis that follows.

Also, According to Casewell et al. (2009), the WD LB 5959 (#659494049367276544) – that sits within the well-defined cooling sequence, at an absolute G magnitude equal to 11.74 and (G_{BP} − G_{RP})$_0$ = −0.18 – is a radial velocity variable. However, they could not find compelling direct evidence of any cool companion from other observational datasets. Follow-up observations presented by Casewell et al. (2012) confirmed the radial velocity variability, leading to the conclusion that the probable companion is a 25–30 M_{Jup} T dwarf. We find that all *Gaia* DR2 parameters for this objects – and in particular the estimated errors in magnitudes – do not show any indication of this being a binary system.

We have also highlighted with an open circle the object EGGR 59, that is a known magnetic WD with field strength of approximately 3 MG (Casewell et al. 2009; Ferrario, de Martino & Gänsicke 2015). This WD lies well within the combined Hyades–Praesepe cooling sequence, and we will retain it in our analysis. We notice that omitting this object from the analysis that follows would not alter the main results of this paper.

Table 1 summarizes parallaxes (with the zero-point correction applied), their fractional errors, absolute magnitudes in the G filter (M_G), as well as the dereddened (G_{BP} − G_{RP})$_0$ colours and associated 1σ errors (taking into account also the errors on the parallax) for the nine known Praesepe WDs considered in our analysis.

3 ANALYSIS

Masses and cooling times of the Praesepe WDs listed in Table 1 have been determined as described in Paper I for the Hyades sample. Interpolations amongst the Salaris et al. (2010) cooling tracks shown in Fig. 1 to match M_G and (G_{BP} − G_{RP})$_0$ of each individual WD, provide mass and cooling age (M_f and t_{cool}), reported in Table 1. The associated errors have been estimated by generating for each object one thousand synthetic M_G and (G_{BP} − G_{RP})$_0$ pairs, with Gaussian distributions (assumed to be independent) centred around the measured values, and 1σ widths equal to the errors on these quantities reported in Table 1. Mass and cooling times for each synthetic sample were determined from the WD tracks, and the 68 per cent confidence limits calculated.

These formal errors on both M_f and $\log(t_{cool})$ are 2–3 times larger than for the Hyades WDs, because of larger error bars on M_G and (G_{BP} − G_{RP})$_0$, but still comparable to the typical errors obtained when employing spectroscopic measurements of $g − T_{eff}$ pairs (see e.g. Cummings et al. 2018, for a recent analysis).

As for the Hyades WDs of Paper I, all Praesepe WDs in this sample have evolved beyond the luminosity range where neutrino energy losses dominate, but have not yet started crystallization. Derivation of M_f and t_{cool} employing the independent CO WD models by Fontaine, Brassard & Bergeron (2001) and Renedo et al. (2010)[2] provide masses unchanged compared to the values in Table 1. As for the case of the Hyades WDs, cooling times obtained with Fontaine et al. (2001) models are the same as the values of Table 1, whilst Renedo et al. (2010) models provide values of t_{cool} within just $d\log(t_{cool})$ = ± 0.02 of the results in Table 1. These small differences have a minor impact on the values of M_i derived in the next section.

Regarding the new WD #662998983199228032, given that we do not have spectroscopic information, we determined its mass and cooling age M_f and t_{cool}, by employing both H-atmosphere and He-atmosphere ($M_{He}/M_{WD} = 10^{-3.5}$) WD tracks from Salaris et al. (2010). This object has a parallax (after zero-point correction) $\pi = 5.201 \pm 0.261$ mas, $M_G = 11.8 \pm 0.04$ (including also the contribution of the parallax error), and colour (G_{BP} − G_{RP})$_0$ = −0.16 ± 0.02. Fig. 2 displays the best fit interpolated DA and DB tracks compared to the CMD of the object. If this WD is of DA spectral type, we derive $\log(t_{cool}) = 8.50 \pm 0.04$ (age in years) and $M_f = 0.80 \pm 0.04$ M$_\odot$. In case of DB spectral type we obtain $\log(t_{cool}) = 8.60 \pm 0.04$ and $M_f = 0.73 \pm 0.05$ M$_\odot$. Given these non-negligible uncertainties especially on the cooling times, due to the unknown spectral type, we won't include this object in the IFMR analysis that follows, although for the sake of comparison we will show its position in the M_f versus M_i diagram in Section 4, assuming it is of DA type like the other cluster WDs.

Fig. 3 compares our determination of WD masses and cooling times with the results by Catalán et al. (2008) – hereafter C08 – and Cummings et al. (2018) – hereafter C18. These two independent

---

[1]https://gea.esac.esa.int/archive/documentation/GDR2/

[2]Using the same bolometric corrections employed for the reference Salaris et al. (2010) models. See Paper I for a brief discussion on the main differences between these two sets of models and the Salaris et al. (2010) calculations.

Table 1. Data about the nine known DA Praesepe WDs shown in Fig. 1, after discarding EGGR 61 and EGGR 60 (see text for details). We display, from left to right, WD name, `Identifier: Gaia DR2`, parallax (in mas), parallax fractional error, absolute G magnitude with error (including the contribution from the parallax error), colour with associated error, logarithm of the cooling time (in years) and error, mass (in solar units), and associated error.

| Name (1)	Identifier: Gaia DR2 (2)	π (3)	σ_π/π (4)	$M_G \pm \sigma$ (5)	$(G_{BP} - G_{RP})_0 \pm \sigma$ (6)	$\log(t_{cool}) \pm \sigma$ (7)	$M_f \pm \sigma$ (8)
LB 5893	661270898815358720	5.447	0.040	11.27 ± 0.04	−0.34 ± 0.02	8.10 ± 0.03	0.87 ± 0.04
EGGR 59	664325543977630464	5.422	0.040	11.58 ± 0.05	−0.19 ± 0.03	8.40 ± 0.04	0.75 ± 0.04
LB 1876	661353224747229184	5.850	0.035	11.63 ± 0.03	−0.22 ± 0.02	8.40 ± 0.02	0.81 ± 0.02
LB 5959	659494049367276544	5.287	0.043	11.74 ± 0.05	−0.18 ± 0.02	8.48 ± 0.02	0.81 ± 0.04
WD 0840+190	661010005319096192	5.135	0.047	11.81 ± 0.03	−0.13 ± 0.02	8.42 ± 0.02	0.76 ± 0.02
WD 0833+198	662798086105290112	5.145	0.039	11.42 ± 0.03	−0.22 ± 0.02	8.31 ± 0.02	0.73 ± 0.02
WD 0840+205	661841163095376896	5.376	0.035	11.90 ± 0.03	−0.11 ± 0.02	8.61 ± 0.03	0.78 ± 0.02
WD 0837+218	665139697978259200	5.185	0.039	11.51 ± 0.07	−0.17 ± 0.03	8.39 ± 0.04	0.69 ± 0.05
LB 8648	660178942032517760	5.370	0.040	11.81 ± 0.03	−0.13 ± 0.02	8.54 ± 0.02	0.77 ± 0.03
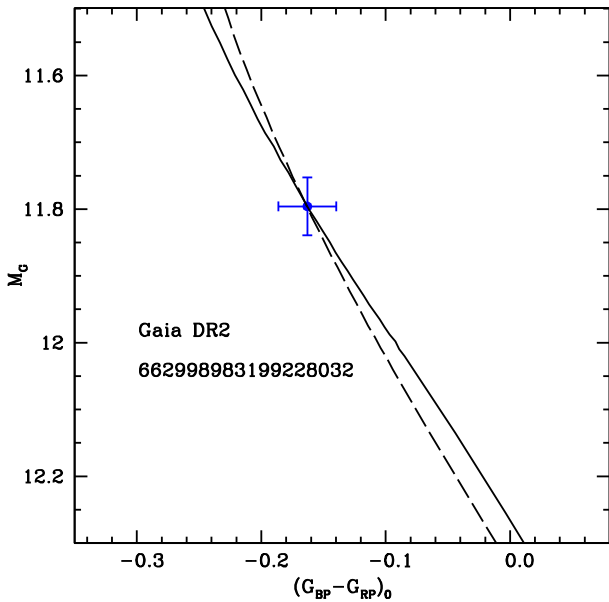
Figure 2. Best fit interpolated DA and DB cooling tracks for the new Praesepe WD #662998983199228032 (see text for details). Error bars include the DR2 quoted photometric errors and the contribution from the parallax error.

Figure 3. Comparison of t_{cool} (upper panels) and M_f (lower panels) between our results of Table 1 and the corresponding values from C18 (left) and C08 (right), respectively. The solid lines display the 1:1 relationship between the quantities on the horizontal and vertical axis.

studies employ g and T_{eff} values for individual WDs from different spectroscopic sources (see the papers for details), and make use of the Salaris et al. (2000) and Fontaine et al. (2001) WD cooling tracks, respectively. We have verified that also Salaris et al. (2000) models agree with the Salaris et al. (2010) ones in terms of luminosity and T_{eff} time evolution for a given WD mass, in the relevant luminosity range. Any difference in the M_f and t_{cool} compared to our analysis is therefore due to inconsistencies between the g-T_{eff} pairs obtained from the WD spectroscopy, and the CMD location of the WD sample.

All objects in our final WD sample (Table 1) are also in C08 study, whereas C18 include five objects common to our sample (LB 1876, LB 5959, WD 0840+190, WD 0833+198, LB 8648). On average C08 results are in agreement with ours, both in terms of M_f and t_{cool}. The most discrepant WD regarding t_{cool} is the magnetic WD EGGR59, whose cooling time determined by C08 is about a factor of 2 lower than our determination. Differences for the other objects
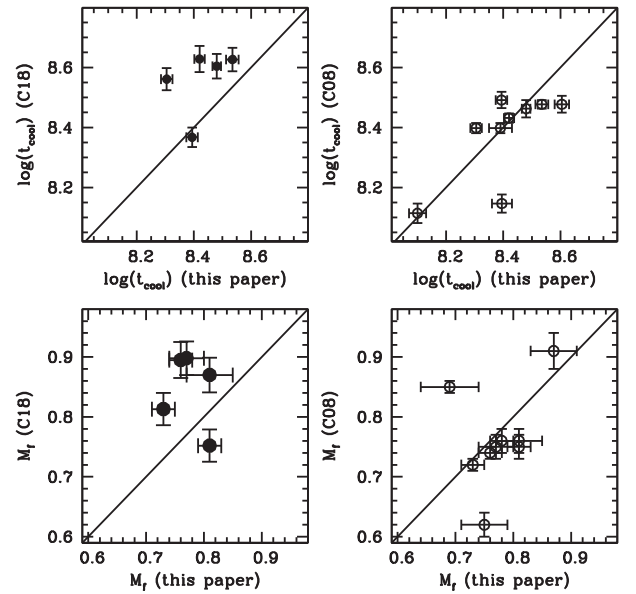
are smaller; for several objects cooling times are in agreement with ours within the errors.

There is also only one object in C08 whose M_f value is substantially higher than what we found, namely WD0837+218. C08 determined for this WD $M_f = 0.85 \pm 0.01$ M$_\odot$, whilst we obtain 0.69 ± 0.05 M$_\odot$. On the other hand, four out of five WDs in C18 sample display longer cooling times and higher masses than in our analysis, namely LB 5959, WD 0840+190, WD 0833+198, and LB 8648.

4 THE INITIAL–FINAL MASS RELATION

As discussed in the Introduction, having determined WD masses and cooling ages from the CMD, we need a cluster age from the MS turn-off to determine the initial values M_i for our WD sample.

Gaia Collaboration (2018) determined a turn-off age $\log(t_{cl}) = 8.85^{+0.08}_{-0.06}$ (t_{cl} in years) obtained from *Gaia* DR2 photom-

Table 2. Initial and final masses for the nine DA WDs of Table 1. From left to right we display the WD name, the initial mass (in solar masses), the asymmetric error bars estimated from the cooling times, and the final mass with associated error (in solar masses – see Table 1).

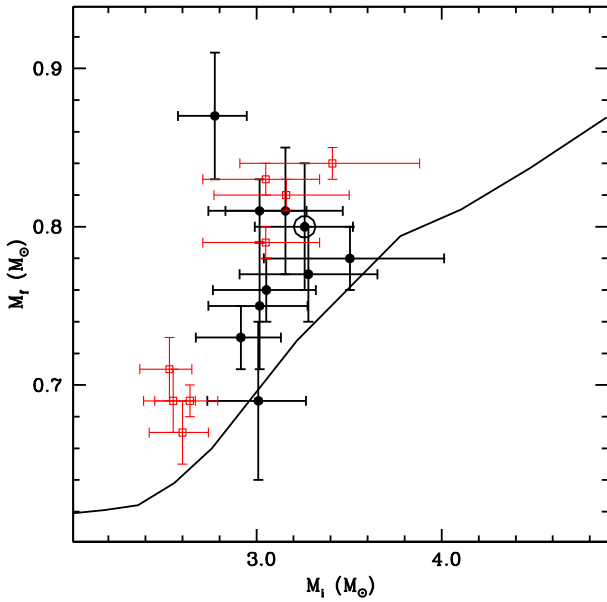| Name	M_i	Δ^-	Δ^+	$M_f \pm \sigma$
LB 5893	2.78	0.20	0.17	0.87 ± 0.04
EGGR 59	3.02	0.28	0.26	0.75 ± 0.04
LB 1876	3.02	0.28	0.25	0.81 ± 0.02
LB 5959	3.16	0.32	0.31	0.81 ± 0.04
WD 0840+190	3.05	0.29	0.27	0.76 ± 0.02
WD 0833+198	2.92	0.24	0.22	0.73 ± 0.02
WD 0840+205	3.50	0.46	0.51	0.78 ± 0.02
WD 0837+218	3.01	0.28	0.26	0.69 ± 0.05
LB 8648	3.28	0.37	0.37	0.77 ± 0.03

Figure 4. IFMR for Praesepe (filled circles with error bars, from Table 2). For the sake of comparison we display also the IFMR for the Hyades derived in Paper I (open squares with error bars). The solid line displays the IFMR from the Marigo et al. (2017) theoretical models. The open circle highlights the new cluster WD #662998983199228032, in case it is of DA spectral type, like the others.

etry and parallaxes, employing the PARSEC (Marigo et al. 2017)[3] isochrones for [Fe/H] = 0.14 – a metallicity consistent with spectroscopic measurements, see e.g. Cummings et al. (2017) and references therein – transformed to the *Gaia* DR2 photometric system. Using this age (and error bar) and – consistently with the cluster age estimate – the initial mass-lifetime values from Marigo et al. (2017) evolutionary tracks, we have determined M_i for our WD sample, as listed in Table 2.

Fig. 4 shows the IFMRs from the data in Table 2, plus the Hyades IFMR from Paper I. As well known, the Hyades cluster has basically the same [Fe/H] of Praesepe (see Cummings et al. 2017, and references therein) and a very similar age (in Paper I we used the

---

[3]Marigo et al. (2017) isochrones are the PARSEC isochrones by Bressan et al. (2012) extended to the end of the thermal pulse phase using the synthetic AGB technique (see the original paper for details).

DR2 determinations for the Hyades age, $\log(t_{cl}) = 8.90^{+0.08}_{-0.06}$, see Gaia Collaboration 2018).

Errors in M_i for Praesepe range between ∼0.2 and ∼0.5 $M_\odot$, with typical values equal to 0.2–0.3 $M_\odot$. Like for the Hyades WDs studied in Paper I, errors on M_i are dominated by the error bar on the cluster age, hence this is essentially a systematic error on all WD initial masses, because increasing or decreasing the cluster age according to its error bar does systematically decrease or increase, respectively, the values of M_i for all WDs of any M_f.

As we discuss below, Hyades and Praesepe IFMRs are in good agreement, but is this agreement preserved when considering the systematic error bars on M_i? For example, if we adopt the lower values of the Hyades WD initial masses and the upper values of Praesepe ones – that means, the upper limit of the Hyades age determination, and the lower limit of Praesepe age according to Gaia Collaboration (2018) – there is clearly a systematic shift between the two IFMRs. However, the errors on the Hyades and Praesepe ages that are determined by the uncertainty in fitting the sparsely populated turn-offs (Gaia Collaboration 2018), cannot be considered independently.

For example, the upper age limit for Praesepe is larger than the lower age limit for the Hyades, but Praesepe cannot be older than the Hyades, when looking at the top panel of Fig. 5, where the CMDs (distance and reddening corrected) of the two clusters are superimposed, together with the best-fitting isochrones from Gaia Collaboration (2018). Praesepe turn-off absolute magnitude is clearly not fainter than the Hyades one.

Instead, when considering the errors on the cluster ages, the difference between the best-fitting ages of Hyades and Praesepe should be preserved. As a consequence, if we consider for example the lower limits of the M_i values for the Hyades given by their error bars – that is, if we consider the upper limit of the Hyades age determination – we should at the same time consider also the lower limit of Praesepe initial masses.

Bearing in mind this discussion on the cluster ages' errors, Fig. 4 shows that the IFMRs of these two clusters appear broadly consistent, even when considering the error bars on M_i. The only discrepant object is Praesepe WD LB 5893, with $M_i = 2.78^{+0.17}_{-0.20}$ for a WD mass $M_f = 0.87 \pm 0.04$ – see also Fig. 1 for its *anomalous* position along the cooling sequence. Even if we neglect LB 5893, and as noticed in Paper I for the Hyades WDs alone, there is a hint of a small spread in the values of M_f, for initial masses around 3 $M_\odot$. Notice that the IFMR of the new WD #662998983199228032 (that we do not consider in the analysis that follows) is consistent with the bulk of the other WDs, if it is assumed to be of spectral type DA like the others.

To quantify better the general agreement between the two cluster IFMRs, we considered M_i and M_f values for Praesepe WDs, the error bars on M_f reported in Table 2, and the random errors on M_i due to the error on the WD cooling times only. For the Hyades we considered the same quantities, as obtained from the data in Paper I. Typical random errors on M_i are 0.01 $M_\odot$ for the Hyades, and just a few hundredths of solar masses for Praesepe WDs. A linear fit to the $M_i - M_f$ data for both clusters (17 WDs), and considering errors on both axis,[4] provides a slope $\Delta M_f / \Delta M_i = 0.20 \pm 0.02$. Discarding the Praesepe WD LB 5893 does not change the result within the errors. If we then consider only the Hyades sample of eight objects, we obtain $\Delta M_f / \Delta M_i = 0.21 \pm 0.02$, consistent with the full sample. Also the zero points are consistent within the

---

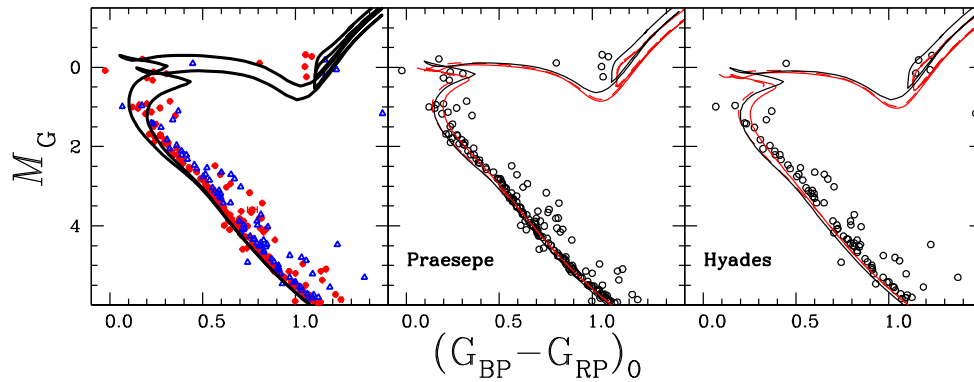[4]We used the routine *fitexy* from Press et al. (1992).

Figure 5. *Gaia* DR2 CMDs of the Hyades (blue empty triangles) and Praesepe (red filled circles), together with – black solid lines– the best-fitting Marigo et al. (2017) isochrones for log(t) = 8.85 and log(t) = 8.90 (left-hand panel – see text for details). In the middle and right-hand panels we display separately Praesepe and Hyades CMDs together with the best-fitting PARSEC isochrones (black solid lines) . The red dashed and solid lines in the middle and bottom panels display non-rotating and rotating MIST isochrones, respectively. In case of Praesepe MIST isochrones have ages equal to log(t) = 8.80 (non-rotating) and log(t) = 8.82 (rotating), whilst for the Hyades MIST isochrones have ages equal to log(t) = 8.85 (non-rotating) and log(t) = 8.87 (rotating – see text for details).

errors when considering the Hyades sample (0.16 ± 0.05 $M_\odot$) and the combined Hyades + Praesepe one (0.20 ± 0.05 $M_\odot$). This agreement of the IFMR for the two clusters is preserved also when considering the lower or the upper limits on M_i for the two clusters (see previous discussion about the error bar on the cluster ages).

The theoretical IFMR by Marigo et al. (2017) is also displayed in Fig. 4. The slope within the lower and upper M_i limits for Hyades and Praesepe WDs is slightly shallower than the data ($\Delta M_f / \Delta M_i$ ~ 0.13), and on the whole this theoretical IFMR underestimates M_f for the initial mass range covered by these two clusters, even when considering the systematic error bars on M_i.

We have also tested the self-consistent use of an independent set of stellar evolution calculations. To this purpose we have downloaded MIST stellar evolution tracks and isochrones (Choi et al. 2016) for [Fe/H] = 0.14, from the web-interpolator of the MIST stellar evolution data base,[5] with (initial linear and angular velocities equal to 40 per cent of the critical values) and without rotation, and compared these isochrones with the best-fitting Marigo et al. (2017) isochrones employed by Gaia Collaboration (2018) to determine Hyades and Praesepe ages. This analysis complements and expands upon the work by C18, who compared IFMRs derived using PARSEC a MIST non-rotating isochrones for their star cluster sample, including Hyades and Praesepe.

Fig. 5 displays this comparison, together with the *Gaia* DR2 CMDs of the Hyades and Praesepe. We show the MIST isochrones that match the MS turn-off luminosity of the Marigo et al. (2017) counterpart. We remark that it is not the purpose of this paper to discuss the age-determination for these two clusters, but just to select the age of MIST isochrones that match the turn-off absolute G magnitude of the best-fitting isochrones determined by Gaia Collaboration (2018).

We find that the cluster ages obtained by Gaia Collaboration (2018) would be 0.05 dex (about 80 Myr) and 0.03 dex (about 50 Myr) younger when using the non-rotating and rotating MIST isochrones, respectively.[6] With these ages we then employed the

[5] http://waps.cfa.harvard.edu/MIST/
[6] Error bars on the MIST cluster ages are the same as in Gaia Collaboration (2018), because age differences between isochrones with the same turn-off absolute magnitudes are constant within the age ranges spanned by Gaia Collaboration (2018) error bars.
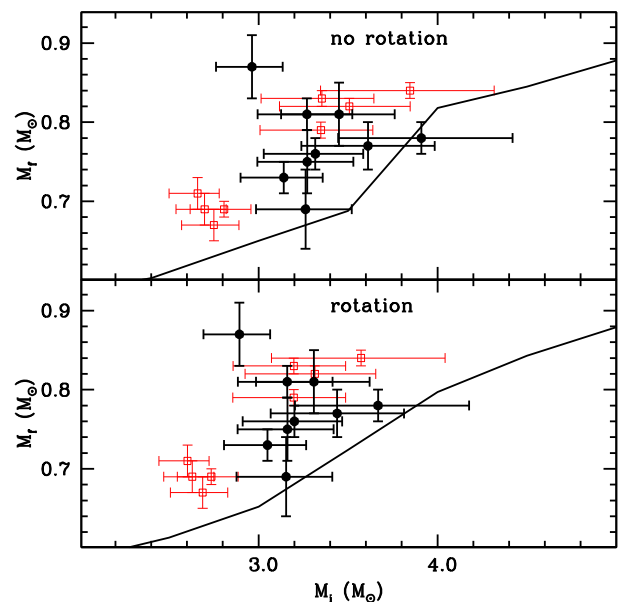

Figure 6. As Fig. 4, but considering cluster ages and progenitor lifetimes from the Choi et al. (2016) models with (lower panel) and without (upper panel) the inclusion of rotation. Solid lines denote the corresponding theoretical IFMRs.

MIST initial mass-lifetime values from Choi et al. (2016) calculations, and the cooling times derived above, to determine M_i values and the IFMR of Hyades and Praesepe.

Compared to the reference IFMR of Fig. 4, the MIST based IFMRs display M_i values typically larger at a given WD mass, with differences varying from object to object and also from cluster to cluster. On average, initial masses M_i are larger by ~ 0.10–0.15 $M_\odot$ for both Hyades and Praesepe when considering the rotating MIST models, while these differences increase to on average ~ 0.2–0.3 $M_\odot$ with the non-rotating models. Fig. 6 shows the resulting IFMRs, compared to the theoretical counterpart obtained from the same calculations. Also in case of using self-consistently MIST models, the theoretical IFMR on average underpredicts the WD masses, even considering the systematic errors on M_i due to the relatively large errors on the cluster ages. The slopes of the semi-

empirical IFMR – calculated as described before – are slightly changed compared to the case of the reference IFMR only for the case of non-rotating models. When considering just the Hyades sample, rotating MIST models give $\Delta M_f/\Delta M_i = 0.19 \pm 0.01$, whilst this slope becomes $\Delta M_f/\Delta M_i = 0.18 \pm 0.01$ for the combined Hyades + Praesepe sample. Non-rotating MIST models give instead $\Delta M_f/\Delta M_i = 0.15 \pm 0.01$ for the Hyades and $\Delta M_f/\Delta M_i = 0.14 \pm 0.01$ for the two clusters combined. These are slightly shallower slopes than the reference IFMR. As for the reference IFMR, the zero points are consistent between the Hyades only and the Hyades + Praesepe samples, for both rotating and non-rotating MIST models.

4.1 Praesepe and Hyades IFMR employing C18 cluster parameters

The recent analysis by C18 has derived Hyades and Praesepe ages – obtained by *BV* CMD fitting employing both PARSEC and non-rotating MIST isochrones – with a much smaller formal error compared to Gaia Collaboration (2018) results. C18 distance moduli and [Fe/H] for both clusters are consistent with Gaia Collaboration (2018), the only difference being $E(B - V) = 0$ for Praesepe[7] – the *traditional* value for Praesepe – instead of $E(B - V) = 0.027$ (see also Cummings et al. 2017). Hyades and Praesepe ages determined with the PARSEC models by C18 are equal to 700 ± 25 Myr and 705 ± 25 Myr, respectively. When using non-rotating MIST models C18 give 705 ± 50 Myr for the Hyades and 685 ± 25 Myr for Praesepe. Notice that C18 ages are typically younger than our adopted values for the Hyades, whereas they are the same or older for Praesepe, but always within the large error bars of the ages based on the *Gaia* DR2 parallaxes and CMDs.

Following the referee suggestion we have rederived the IFMR for both Hyades and Prasepe using C18 results, *Gaia* DR2 WD parallaxes and photometry, employing both PARSEC and non-rotating MIST models to determine progenitor ages and masses. This will enable us to make a fully consistent comparison with C18 IFMR results that made use of spectroscopic estimates of WD masses and cooling times.

Hyades WD masses and cooling times from *Gaia* DR2 are unchanged compared to the results of Paper I, but this is not the case for Praesepe. A zero reddening instead of $E(B - V) = 0.027$ implies redder and fainter WDs compared to the results in Table 1. To give an idea of the magnitude of this effect, the reddening law by Gaia Collaboration (2018) gives, in the colour range of Praesepe WDs, $A_G \sim 3.1\, E(B - V)$, and $E(G_{BP} - GRP) \sim 1.7 E(B - V)$. Fig. 7 compares the distance and reddening corrected CMD of the nine Praesepe WDs employed in our IFMR determination, with the CMD of the same objects but in case of $E(B - V) = 0$. Assuming zero reddening for Praesepe as in C18 causes a systematic decrease of the derived WD masses (by 0.02–$0.05\,M_\odot$), and a systematic increase of their cooling ages (by 0.06–0.30 dex) compared to the values reported in Table 1, as shown in Fig. 8

By employing C18 cluster ages we have then determined the Hyades and Praesepe IFMRs, with both PARSEC and non-rotating MIST models. Table 3 summarizes the results, that are also displayed in Fig. 9.

---

[7]Our Paper I and C18 employ $E(B - V) = 0.0$ for the Hyades. A zero reddening for the Hyades is confirmed also by the recent Taylor (2006) analysis.
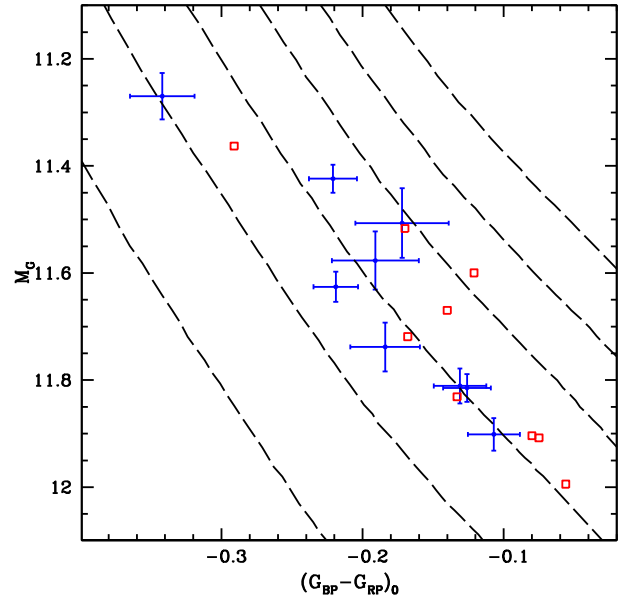
Figure 7. As Fig. 1, but showing just the nine Praesepe WDs employed to determine the IFMR, together with the adopted cooling tracks. Dots with error bars display the WD CMD when employing the reference reddening $E(B - V) = 0.027$, while open squares (without error bars, for the sake of clarity) display the CMD assuming zero reddening, following C18 analysis (see text for details).
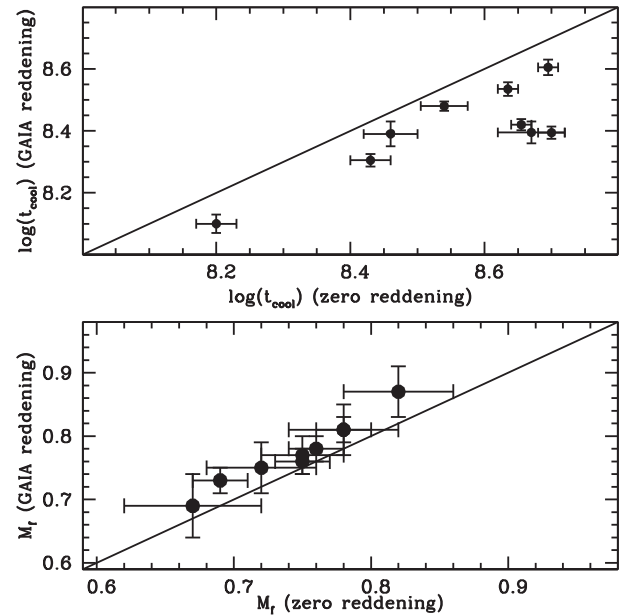

Figure 8. As Fig. 3, but comparing the results in Table 1 with WD masses and cooling times obtained assuming zero reddening for Praesepe.

Both cluster IFMRs have now smaller errors associated with M_i, reflecting the much reduced error on the cluster ages. The Hyades IFMR is similar to our results in Figs 4 and 6 (see also Paper I), with just a small systematic increase of M_i by 0.1–$0.4\,M_i$, due to the lower adopted cluster age. The result is however within the error bars of Figs 4 and 6.

The situation is quite different for Praesepe. Both M_i and, to a smaller degree, M_f values are reduced compared to the results in Figs 4 and 6. The large reduction of M_i values is mainly due

Table 3. As Table 2 but for Praesepe and Hyades IFMRs obtained adopting cluster ages and reddenings from C18 (see text for details).

| Name	M_i	Δ^-	Δ^+	$M_f \pm \sigma$
Praesepe				
LB 5893	2.84	0.05	0.05	0.82 ± 0.04
EGGR 59	3.85	0.30	0.44	0.72 ± 0.04
LB 1876	4.07	0.23	0.28	0.78 ± 0.02
LB 5959	3.30	0.12	0.14	0.78 ± 0.04
WD 0840+190	3.76	0.15	0.17	0.75 ± 0.02
WD 0833+198	3.08	0.08	0.08	0.69 ± 0.02
WD 0840+205	4.03	0.20	0.23	0.76 ± 0.02
WD 0837+218	3.13	0.09	0.11	0.67 ± 0.05
LB 8648	3.65	0.14	0.15	0.75 ± 0.03
Hyades				
HZ 14	2.64	0.03	0.03	0.71 ± 0.02
LAWD 19	2.68	0.03	0.04	0.69 ± 0.02
HZ 7	2.73	0.04	0.04	0.67 ± 0.02
LAWD 18	2.78	0.04	0.04	0.69 ± 0.01
HZ 4	3.33	0.08	0.09	0.79 ± 0.01
EGGR 29	3.34	0.08	0.09	0.83 ± 0.01
HG 7–85	3.50	0.10	0.11	0.82 ± 0.01
GD 52	3.88	0.14	0.17	0.84 ± 0.01
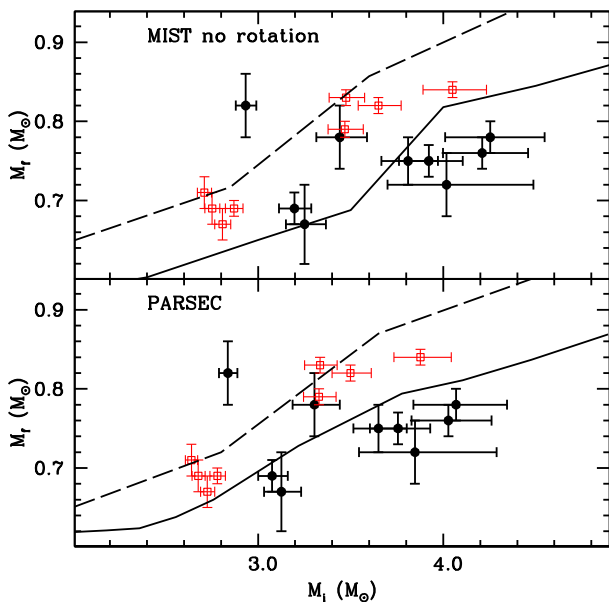
Figure 9. As Fig. 6, but showing our IFMRs derived using ages and reddenings from C18. The dashed lines display C18 analytical IFMRs determined using PARSEC models (lower panel) and non-rotating MIST models (upper panel), whilst solid lines show the theoretical IFMRs predicted by PARSEC and MIST models (see text for details).

to the sizably longer WD cooling times compared to the results in Table 1. There is now an average offset between Praesepe and Hyades IFMR, with Praesepe IFMR on average shifted towards larger values of M_i at fixed M_f. This is inconsistent with C18 results and our IFMRs determined employing Gaia Collaboration (2018) cluster parameters.

This difference between Hyades and Praesepe IFMRs is a consequence of the assumption of zero reddening for Praesepe, and is not due to the cluster ages determined by C18. If we employ just C18

cluster ages but Praesepe WD masses and cooling times of Table 1, we still have consistency between Hyades and Praesepe IFMRs.

Fig. 9 displays also the analytical IFMRs by C18 obtained with both PARSEC and non-rotating MIST models. These C18 IFMRs show only a small offset (by ∼0.1 M⊙) towards smaller M_i values at fixed M_f when compared to our Hyades results. This is mainly due to the slightly longer cooling times we obtain for the Hyades WDs, compared to C18. Praesepe results are instead completely inconsistent with C18 IFMRs.

When compared to the theoretical counterparts from PARSEC and non-rotating MIST models – also displayed in Fig. 9– our semi-empirical Hyades results predict larger M_f values for the initial mass range covered by the cluster. This is in agreement with C18 and our IFMRs in Figs 4 and 6. In case of Praesepe most of the WDs now lie below the theoretical IFMRs in Fig. 9, implying lower M_f values than predicted from theory.

The reddening adopted for Praesepe is therefore crucial to establish photometrically the cluster IFMR. The value of $E(B - V) = 0.027$ determined by Gaia Collaboration (2018) from isochrone fitting is in agreement with independent estimates by Taylor (2006). When employing this reddening and the extinction law from Gaia Collaboration (2018), the Praesepe IFMR is consistent with the Hyades result. Assuming the traditional zero reddening for the *Gaia* CMD of Praesepe WDs, induces a very large dispersion in the global IFMR obtained from these two clusters that are almost coeval and with the same metallicity.

5 SUMMARY AND DISCUSSION

We have employed the *Gaia* DR2 sample of *bona fide* Praesepe member stars, and selected the objects on the WD cooling sequence. 10 out of a total of 12 WDs – all of spectral type DA – satisfy the quality criteria selected from the quality indicators available in *Gaia* DR2. Nine objects are already known DA WDs, the remaining one is a new WD member, with DR2 identifier #662998983199228032. A spectroscopic follow-up is needed to establish the spectral type of this new object.

We have determined masses and cooling times of the WDs by matching their CMD (corrected for reddening and distance using reddening and parallaxes from Gaia Collaboration 2018) with theoretical cooling sequences. The accuracy of DR2 parallaxes (∼4 per cent fractional errors) and photometry (errors of a few hundredths of a magnitude) has allowed us to determine masses with an average error of 3–5 per cent, and cooling times with an average uncertainty of 5–7 per cent. For the new WD of unknown spectral type, we derive two pairs of cooling time-mass values, namely $\log(t_{cool}) = 8.50 \pm 0.04$, $M_f = 0.80 \pm 0.04$ M⊙ from DA tracks, and $\log(t_{cool}) = 8.60 \pm 0.04$ and $M_f = 0.73 \pm 0.05$ M⊙ from DB tracks.

An IFMR for the confirmed DA Praesepe WDs in our sample has been then determined by assuming the cluster MS turn-off age (∼710 Myr) recently determined from the *Gaia* DR2 cluster CMD and PARSEC stellar evolution models (Gaia Collaboration 2018). This Praesepe IFMR is consistent with the Hyades IFMR derived in Paper I from DR2 data and the same methods applied here. We have also derived self-consistently Praesepe and Hyades IFMRs employing two alternative sets of stellar evolution models, the non-rotating and rotating MIST models. The use of MIST models shifts the individual M_i values towards higher values compared to the reference PARSEC results, due to a different progenitor mass–lifetime relationship, and the typically younger ages derived with MIST models. The magnitude of these shifts depend on whether the non-rotating

(increase by 0.20–0.30 $M_\odot$) or rotating (increase 0.10–0.15 $M_\odot$) MIST models are employed.

In these IFMR determinations, the Praesepe WD LB 5893 appears to deviate from the rest of the objects in the $M_i - M_f$ diagram, resulting too massive for its derived M_i. This is consistent with its *anomalous* location along the cooling sequence (see Fig. 1), and confirms previous findings (see Claver et al. 2001; Casewell et al. 2009) based on spectroscopic $g - T_{eff}$ determinations. As discussed in Casewell et al. (2009), there is nothing peculiar about this object, for neither magnetic fields nor rapid rotation was detected. These authors speculate whether it may have formed from a blue straggler star, given the known presence of blue stragglers in this cluster (e.g. Fossati et al. 2010, and references therein). Obviously strong differential mass-loss is also a possibility, even though among the known cluster WDs we see such a strong effect only for this single object. We also notice that this star is the most massive WD detected so far in Praesepe, and is located near the cluster centre. It is possible that close interactions between massive stars in the denser cluster core might have affected the IFMR for this WD.

Two other interesting objects are LB 5959 and EGGR 59. Regarding LB 5959, we have already mentioned in Section 2 that Casewell et al. (2012) observations suggest the presence of a companion with mass equal to 25–30 M_{Jup}, although *Gaia* DR2 parameters are consistent with this object being a single star. In the scenario envisaged by Casewell et al. (2012) the substellar companion must have been engulfed by the WD progenitor during the AGB evolution. This common envelope interaction may therefore have modified the IFMR of this object, compared to our estimates based on single-star evolution for the progenitor.

As for the magnetic WD EGGR 59, the origin of WDs with strong magnetic fields is still debated (see e.g. Ferrario et al. 2015; García-Berro, Kilic & Kepler 2016, for reviews). These fields might be fossil, the remnants of original weak magnetic fields amplified during the course of the evolution of the progenitor (Angel, Borra & Landstreet 1981). According to a competing scenario (Tout et al. 2008), all highly magnetic white dwarfs (defined as WDs with fields in excess of 1 MG, like EGGR 59), both single stars or the components of magnetic cataclysmic variables, have instead a binary origin. Interestingly, also EGGR 59 is located in the cluster central region, where interactions between stars are more likely.

As shown in Fig. 1, this star sits nicely within the Praesepe cooling sequence; assuming that magnetic fields do not affect the WD mass-radius relation and the bolometric corrections for the *Gaia* photometric filters, its mass is fully consistent with the general IFMR of the other non-magnetic WDs. Regarding the WD mass-radius relation, a fundamental problem is that the surface magnetic field of a star does not necessarily reflect the internal field. According to the models by Suh & Mathews (2000), very high internal magnetic fields, of the order of 10^{11}–10^{13} G, can modify the non-magnetic mass-radius relation, resulting in increased radii at fixed WD mass. This would cause an underestimate of the WD mass from CMD analyses, when non-magnetic WD models are employed. On the other hand, assuming the mass-radius relation is unaffected by the internal (unknown) magnetic field strength, a recent study by Külebi et al. (2013), who applied magnetized WD spectra to infer mass and cooling times of this object, found that within the errors of their diagnostics this WD does not significantly deviate from the mean IFMR of non-magnetized WDs. If this result is confirmed by more comprehensive analyses of the effect of magnetic fields on WDs (both evolutionary and spectral properties), it could help constraining the scenario for magnetic WD formation.

The comparison of our Hyades + Praesepe IFMR with theoretical predictions also discloses – confirming an analogous result by C18 (see their Fig. 5) – a systematic discrepancy between theoretical IFMR predictions and the semi-empirical results. Both PARSEC and MIST (rotating and non-rotating) calculations – that include the full AGB evolution – on average do underpredict the final WD masses in the initial mass range covered by these clusters. The size of the discrepancy is of the order of a few 0.01 $M_\odot$, the larger discrepancy found for the IFMR determined with the MIST rotating models. This sets important constraints on the growth of the CO core in AGB stars with these progenitor masses, with implications for the efficiency of mass-loss, third dredge-up, and contribution of AGB stars to the integrated infrared light of stellar populations.

The photometric determination of Praesepe IFMR – and more in general for all *Gaia* clusters with precise parallax and magnitude measurements of their WD populations – relies crucially on the reddening assumed for the cluster. All these results are based on employing for consistency a value $E(B - V) = 0.027$ determined by Gaia Collaboration (2018) from isochrone fitting to the *Gaia* DR2 CMD of MS, turn-off, and core He-burning stars. This value is in agreement with $E(B - V) = 0.027 \pm 0.004$ obtained independently by Taylor (2006).

We have also determined Praesepe WD masses and cooling times employing the traditional zero reddening for Praesepe, as in C18 analysis. In this case WD masses are reduced and cooling times largely increased compared to the case of $E(B - V) = 0.027$. This leads to a very different IFMR (irrespectively of using Gaia Collaboration 2018, or C18 cluster age estimates) that is on average shifted to larger M_i values compared to the Hyades, implying a large dispersion in the IFMR even for two clusters with the same metallicity and approximately the same age.

REFERENCES

Agertz O., Kravtsov A. V., 2015, ApJ, 804, 18
Angel J. R. P., Borra E. F., Landstreet J. D., 1981, ApJS, 45, 457
Anthony-Twarog B. J., 1984, AJ, 89, 267
Bressan A., Marigo P., Girardi L., Salasnich B., Dal Cero C., Rubele S., Nanni A., 2012, MNRAS, 427, 127
Casewell S. L. et al., 2012, ApJ, 759, L34
Casewell S. L., Dobbie P. D., Napiwotzki R., Burleigh M. R., Barstow M. A., Jameson R. F., 2009, MNRAS, 395, 1795
Catalán S., Isern J., García-Berro E., Ribas I., 2008, MNRAS, 387, 1693 (C08)
Choi J., Dotter A., Conroy C., Cantiello M., Paxton B., Johnson B. D., 2016, ApJ, 823, 102
Claver C. F., Liebert J., Bergeron P., Koester D., 2001, ApJ, 563, 987
Cummings J. D., Kalirai J. S., Tremblay P.-E., Ramirez-Ruiz E., 2015, ApJ, 807, 90

Cummings J. D., Deliyannis C. P., Maderak R. M., Steinhauer A., 2017, AJ, 153, 128

Cummings J. D., Kalirai J. S., Tremblay P.-E., Ramirez-Ruiz E., Choi J., 2018, ApJ, 866, 21 (C18)

Dobbie P. D. et al., 2006, MNRAS, 369, 383

Dobbie P. D., Pinfield D. J., Napiwotzki R., Hambly N. C., Burleigh M. R., Barstow M. A., Jameson R. F., Hubeny I., 2004, MNRAS, 355, L39

Dominguez I., Straniero O., Tornambe A., Isern J., 1996, ApJ, 472, 783

Dufour P., Blouin S., Coutu S., Fortin-Archambault M., Thibeault C., Bergeron P., Fontaine G., 2017, in Tremblay P.-E., Gaensicke B., Marsh T., eds, ASP Conf. Ser. Vol. 509, 20th European White Dwarf Workshop. Astron. Soc. Pac., San Francisco, p. 3

Ferrario L., Wickramasinghe D., Liebert J., Williams K. A., 2005, MNRAS, 361, 1131

Ferrario L., de Martino D., Gänsicke B. T., 2015, Space Sci. Rev., 191, 111

Fontaine G., Brassard P., Bergeron P., 2001, PASP, 113, 409

Fossati L., Mochnacki S., Landstreet J., Weiss W., 2010, A&A, 510, A8

Gaia Collaboration, 2018, A&A, 616, A10

García-Berro E., Kilic M., Kepler S. O., 2016, Int. J. Mod. Phys., 25, 1630005

Greggio L., 2010, MNRAS, 406, 22

Holberg J. B., Bergeron P., 2006, AJ, 132, 1221

Iben I., Jr, Renzini A., 1983, ARA&A, 21, 271

Kalirai J. S., Saul Davis D., Richer H. B., Bergeron P., Catelan M., Hansen B. M. S., Rich R. M., 2009, ApJ, 705, 408

Karakas A. I., Lattanzio J. C., 2014, PASA, 31, e030

Külebi B., Kalirai J., Jordan S., Euchner F., 2013, A&A, 554, A18

Lindegren L. et al., 2018, A&A, 616, A2

Marigo P. et al., 2017, ApJ, 835, 77

Press W. H., Teukolsky S. A., Vetterling W. T., Flannery B. P., 1992, Numerical Recipes in FORTRAN. The Art of Scientific Computing. Cambridge Univ. Press, Cambridge

Renedo I., Althaus L. G., Miller Bertolami M. M., Romero A. D., Córsico A. H., Rohrmann R. D., García-Berro E., 2010, ApJ, 717, 183

Salaris M., Bedin L. R., 2018, MNRAS, 480, 3170(Paper I)

Salaris M., García-Berro E., Hernanz M., Isern J., Saumon D., 2000, ApJ, 544, 1036

Salaris M., Serenelli A., Weiss A., Miller Bertolami M., 2009, ApJ, 692, 1013

Salaris M., Cassisi S., Pietrinferni A., Kowalski P. M., Isern J., 2010, ApJ, 716, 1241

Suh I.-S., Mathews G. J., 2000, ApJ, 530, 949

Taylor B. J., 2006, AJ, 132, 2453

Tout C. A., Wickramasinghe D. T., Liebert J., Ferrario L., Pringle J. E., 2008, MNRAS, 387, 897

Tremblay P.-E., Bergeron P., Gianninas A., 2011, ApJ, 730, 128

Weidemann V., 2000, A&A, 363, 647

Williams K. A., Bolte M., Koester D., 2009, ApJ, 693, 355

This paper has been typeset from a TEX/LATEX file prepared by the author.